Articles

NMR Solution Structure of a Two-Disulfide Derivative of Charybdotoxin: Structural Evidence for Conservation of Scorpion Toxin α/β Motif and Its Hydrophobic Side Chain Packing[†,‡]

Jianxing Song, Bernard Gilquin,* Nadège Jamin, Eugenia Drakopoulou, Marc Guenneugues, Marc Dauplais, Claudio Vita, and André Ménez

Département d'Ingénierie et d'Etudes des Protéines, CEA, Saclay, 91191 Gif-sur-Yvette Cedex, France

Received October 30, 1996; Revised Manuscript Received January 2, 1997[⊗]

ABSTRACT: The α/β scorpion fold consisting of a short α-helix and β-sheet is a structural motif common to scorpion toxins, insect defensins, and plant γ-thionins that invariably contains three disulfides. CHABII is a two-disulfide derivative of the scorpion toxin charybdotoxin (ChTX), chemically synthesized by inserting two L-α-aminobutyric acids in place of the two half-cystine residues involved in the disulfide 13−33. This disulfide is one of the two disulfides which connect the α-helix to the β-sheet. The solution structure of CHABII was determined at pH 6.3 and 5 °C using 2D NMR and simulated annealing from 513 distance and 46 dihedral angle constraints. The NMR structure of CHABII is well-defined as judged from the low value of the averaged backbone rms deviation between the 30 lowest energy structures and the energy-minimized mean structure (⟨rmsd⟩ = 0.65 Å for the entire sequence and 0.48 Å for the segment 3−36). Analysis and comparison of the solution structures of CHABII and ChTX lead to the following conclusions: (i) the fold of CHABII is similar to that of ChTX as indicated by the low value of the averaged backbone atomic rms deviation between the 10 lowest energy solution structures of the two proteins (1.44 Å); (ii) the packing of the hydrophobic core is well-preserved, underlying the critical structural role of the hydrophobic interactions even for such a small and cysteine-rich protein as ChTX.

Identification of the interactions that govern protein structure and stability is of fundamental importance to understand, modify, and engineer protein structures and functions. In addition to the well-identified noncovalent interactions—hydrophobic interactions, hydrogen bonds, salt bridges, and weak polar interactions—a number of proteins also possess covalent stabilizing factors, i.e., disulfide bonds. Small proteins (less than 100 residues) often possess several disulfides which are conserved in all members of the protein family and are considered to play an important role in the maintenance of their structure. In order to investigate this role, peptides and proteins in which native disulfides were removed have been the subject of various structural investigations (Le-Nguyen et al., 1993; Mayr et al., 1994; Coles et al., 1994; Eyles et al., 1994; Xu & Nelson, 1994; Chang, 1995; Ferrer et al., 1995). In particular, all two-disulfide derivatives of BPTI have been studied by NMR (van Mierlo et al., 1991) or X-ray crystallography (Eigenbrot et al., 1990). In most of the studies, when one disulfide is deleted, the resulting proteins still present a native-like overall fold although they are usually less stable than the wild-type proteins.

Charybdotoxin (ChTX)[1] is a small protein containing 37 residues, isolated from the venom of the scorpion (*Leiurus quinquestriatus*). It is a member of a family of proteins that adopt the α/β scorpion fold, a three-dimensional structure composed of a short α-helix interacting with a β-sheet (Bontems, 1992; Bontems et al., 1991a,b, 1992). This α/β motif always involves three disulfides which adopt the following cysteine sequence: Cys-[...]-Cys-x-x-x-Cys-[...]-x-x-Cys-[...]-Cys-x-Cys. One disulfide (7−28) links a loop to the β-sheet whereas the other two (13−33 and 17−35) connect the α-helix to the β-sheet. This consensus sequence is found in many functionally different proteins, including scorpion toxins (Bontems et al., 1991b), insect defensins (Bonmatin et al., 1992; Cornet et al., 1995), and plant γ-thionins (Bruix et al., 1993) which all adopt the α/β motif. In other words, this simple, compact and well-organized motif exerts numerous unrelated functions, illustrating its high amino acid sequence permissiveness (Ménez et al., 1992). This motif has been chosen as a versatile scaffold for protein engineering, and indeed new functions have been successfully engineered into it (Vita et al., 1995; Drakopoulou et al., 1996; Zinn-Justin et al., 1996).

To further exploit this scaffold, the role of its disulfides needs to be explored. Therefore, each one of the three

[†] This work received support from DRET.

[‡] The atomic coordinates of CHABII have been deposited in the Brookhaven Protein Data Bank (file name 1BAH).

* To whom correspondence should be addressed.

[⊗] Abstract published in *Advance ACS Abstracts,* March 1, 1997.

[1] Abbreviations: Aba, α-aminobutyric acid; BPTI, bovine pancreatic trypsin inhibitor; CD, circular dichroism; ChTX, charybdotoxin; NMR, nuclear magnetic resonance; 2D, two dimensional; COSY, correlated spectroscopy; DQF-COSY, double-quantum-filtered correlated spectroscopy; TOCSY, total correlated spectroscopy; NOE, nuclear Overhauser effect; NOESY, NOE spectroscopy; rmsd, root-mean-square deviation; Z, 5-oxoproline (pyroglutamic acid).

S0006-2960(96)02720-1 CCC: $14.00

disulfides of ChTX has been replaced by a pair of L-α-aminobutyric acids (Aba) which are isosteric to cysteine (Vita et al., 1994). The disulfide 13−33 is of special interest due to its location in the highly structured core of the α/β motif and its participation to the conserved spacing cysteine sequence Cys-x-x-x-Cys-[...]-Cys-x-Cys. It was previously shown that the deletion of this disulfide had little effect on the biological activity and the secondary structure (as judged from circular dichroism experiments) (Vita et al., 1994) of the toxin. These observations are difficult to interpret without the knowledge of the three-dimensional structure of this derivative. In this paper, we report the NMR solution structure of the Cys13Aba, Cys33Aba derivative named CHABII. Analysis of its structure allowed us to address the following two questions. Is the overall fold of this derivative affected upon deletion of the 13−33 disulfide? Does this deletion modify the packing of the hydrophobic core which has been previously suggested to participate to the stabilization of the toxin fold (Bontems et al., 1992)?

MATERIALS AND METHODS

Sample Preparation. CHABII was chemically synthesized and purified as described previously (Vita et al., 1994). The sample for NMR measurements was prepared by dissolving 3 mg of CHABII in 0.4 mL of a mixture of either 90% (v/v) H_2O and 10% (v/v) D_2O or pure D_2O to give a final concentration of 1.5 mM. Since CD analysis indicates that CHABII unfolds below pH 6.0, pH (or pD) 6.3 was chosen for NMR experiments used for 3D structure determination, without correcting for the isotope effect. Chemical shifts were measured relative to 3-(trimethylsilyl)[2,2,3,3-$^2H_4$]-propionate (TSP-d_4) used as an internal reference.

NMR Experiments. NMR experiments were performed on Bruker AMX600 and AMX500 spectrometers, at pH 6.3 and different temperatures (5, 15, and 25 °C). In order to compare the Hα chemical shifts of CHABII and ChTX at pH 6.3, one set of NOESY and TOCSY experiments were performed on ChTX at 15 °C rather than at 5 °C due to broadening of resonances.

NMR spectra were obtained in the phase-sensitive, absorption mode with the hypercomplex method (States et al., 1982). The spectra were acquired with 512 (t_1) × 1024 (t_2) points, except 1024 (t_1) × 2048 (t_2) points for the DQF-COSY. Homonuclear NMR experiments were collected using standard methods: TOCSY (Braunschweiler & Ernst, 1983; David & Bax, 1985; Shaka et al., 1983; Rance, 1987), DQF-COSY (Piantini et al., 1982; Rance et al., 1983), and NOESY (Kumar et al., 1980; Macura & Ernst, 1980). The water signal was suppressed by applying a 1-1 observation pulse to avoid loss of amide proton resonance intensity due to fast exchange with the solvent (Plateau & Gueron, 1982). In addition, NOESY and DQF-COSY spectra used to extract distance and angle constraints were recorded with the WATERGATE sequence (Piotto et al., 1992; Trimble & Bernstein, 1994).

All NMR data were processed and analyzed on either a Bruker X32 using UXNMR software or a Sun Spark Station using FELIX 2.3 software (Biosym Technologies, San Diego).

Distance and Dihedral Angle Restraints. All interproton distance and torsional angle restraints for structure calculation were derived from NMR data acquired at 5 °C and pH 6.3. NOE cross peaks were extracted from a NOESY spectrum with a mixing time of 150 ms, and their intensities were converted into interproton distances as described previously (Dauplais et al., 1995). $^3J_{NH-H\alpha}$ scalar coupling constants were determined from DQF-COSY spectra. ϕ dihedral angle restraints were calibrated from $^3J_{NH-H\alpha}$ coupling constants using the empirical Karplus relationship (Karplus, 1963; Pardi et al., 1984). For $^3J_{NH-H\alpha}$ greater than 8 Hz, the ϕ backbone dihedral angles were restrained in intervals centered at −120° (from −120° ± 25° to −120° ± 45° according to the observed values of $^3J_{NH-H\alpha}$). χ_1 angle restraints were obtained from the analysis of $^3J_{H\alpha-H\beta}$ coupling constants and intraresidue NOEs (Hyberts et al., 1987). The limits of the intervals for χ_1 were set to ±45°. Additional restraints were included in the distance geometry calculations to define the two disulfides. No hydrogen-bonding restraints were introduced.

3D Structure Calculations. 3D structures were calculated using the distance geometry program DIANA (Guntert et al., 1991) and simulated annealing procedures. A total of 100 structures were generated by DIANA from the final set of experimental restraints. Of these, 46 structures with target functions less than 10 and without distance violations greater than 0.5 Å were further refined by applying an X-PLOR protocol (Brünger et al., 1987; Brünger, 1992). The simulated annealing protocol used here was formulated from one described previously (Gippert et al., 1990) and implemented in our laboratory (Zinn-Justin et al., 1992; Gilquin et al., 1993). The structures were displayed and analyzed on a Silicon D_Graphics 4D/25 station using SYBYL (Tripos Associates Inc.). The criteria for defining hydrogen bonds were a hydrogen−acceptor distance lower than 2.8 Å and a donor−H−acceptor angle larger than 120.0°.

RESULTS

Resonance Assignments and NMR Data. Assignment of NMR spectra of CHABII was achieved according to the well-established sequential assignment method (Wagner & Wüthrich, 1982; Wüthrich, 1986). All spin systems of CHABII, except the N-terminal residue Z1, were observed from amide−proton connectivities in the 2D TOCSY spectra in H_2O at 5 °C and pH 6.3. The sequential assignment of CHABII is shown in Figure 1A, and the chemical shifts are included in Supporting Information. Interestingly, the hydroxyl proton resonances of T3, T23, and S24 were observed (with chemical shifts of 5.98, 5.73, and 5.84 ppm, respectively; see Figure 1B). These observations suggest that these hydroxyl protons are shielded from contact with solvent (Hammen et al., 1995).

In order to estimate the structural similarity between CHABII and the native ChTX, the chemical shifts were compared under the same experimental conditions (pH 6.3 and 15 °C). The CαH chemical shifts were used as they are less sensitive to temperature than those of the amide protons (Wishart et al., 1991). Figure 2 shows that the majority of the chemical shift difference between the two toxins is less than 0.15 ppm. This similarity suggests that the α/β fold is preserved. The only major differences higher than 0.3 ppm are located on Z1, K11, and G26. In order to get structural details, the 3D structure of CHABII was further determined.

Secondary Structure. Analysis of the NMR data (short-range NOEs and $^3J_{NH-H\alpha}$ scalar coupling constants) (Figure 3) indicates that CHABII has a secondary structure similar

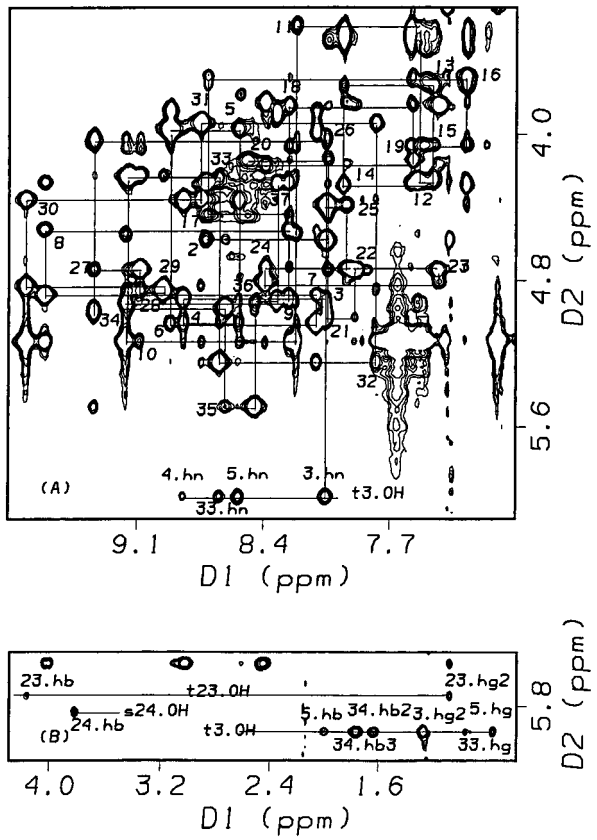

FIGURE 1: (A) NOESY spectrum of CHABII (500 MHz, mixing time of 150 ms) acquired in H_2O at pH 6.3 and 5 °C. The numbers are used to indicate the positions of intraresidual NH/Hα cross peaks. The sequential $d_{\alpha N}$ connectivities are shown for segment 2−37 of CHABII. NOE connectivities between the hydroxyl hydrogen of T3 and the other amide protons are also shown. (B) NOE connectivities between the hydroxyl protons of T3, T23, and S24 and the other side chain protons in the same NOESY spectrum as in (A).

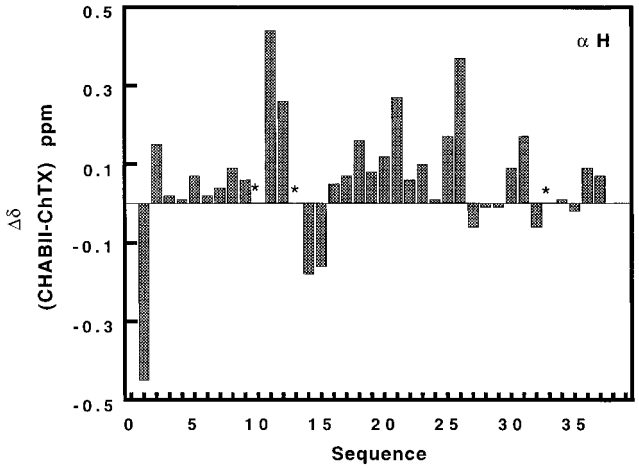

FIGURE 2: Hα chemical shift differences ($\Delta\delta$, ppm) between CHABII and ChTX at 15 °C, pH 6.3. *: not detected (S10) or not compared (between Cys13,33 and Aba13,33).

to that of ChTX. First, the low $^3J_{NH-H\alpha}$ values and $d_{\alpha N(i,i+3)}$ NOEs identify a helical segment running from S10 to L20. However, the weak intensity of several $d_{NN(i,i+1)}$ NOEs over the segment 10−13 and the high $^3J_{NH-H\alpha}$ values of Aba13 and V16 suggest that the helix is somewhat distorted (vide infra). Second, the high $^3J_{NH-H\alpha}$ values and the strong $d_{\alpha N}$ connectivities indicate the presence of three extended strands along the stretches R25−M29, K32−Y36, and F2−T3 as in ChTX.

Quality of the 3D Structures. Three-dimensional structures were computed according to the protocol described in Materials and Methods. A set of 513 distance restraints was used including 220 intraresidue, 125 sequential, 66 medium-range, 92 long-range, and 10 ambiguous restraints, and 6 additional distance restraints derived from the two disulfides. The number and type of NOE connectivities per residue are shown in Figure 4. The average number of distance restraints per residue is equal to 14. Additionally, 30 ϕ and 16 χ_1 dihedral angle restraints were introduced.

Table 1 presents structural statistics of the 30 lowest energy-refined structures. The low values of distance and dihedral restraint energy terms indicate that all these final structures are consistent with the experimental NMR data. No distance violation exceeds 0.3 Å, and no dihedral angle violation exceeds 5°. Moreover, the covalent geometry is respected as evidenced by the low ⟨rmsd⟩ values for the bond lengths (0.012 Å) and valence angles (2.6°). Importantly, the negative value (−23 kcal/mol) of van der Waals energy suggests the absence of any inappropriate nonbonded contacts.

Backbone Structure Description. Figure 5a presents a stereoview of the superimposition of the 30 refined structures fitted with their energy-minimized mean structure. The overall backbone structure is the same for all structures. The average backbone rmsd between the 30 structures and their energy-minimized mean structure is 0.65 Å, clearly indicating that the structures of CHABII calculated from NMR data are well-defined even in the absence of disulfide 13−33. However, some regions of the structure are more precisely defined than others (Figure 5a). In particular, due to the absence of any NOE restraints, the N-terminal residue, Z1, appears to be disordered. Accordingly, the averaged backbone rmsd becomes lower (0.48 Å) along the fragment 3−36.

Helix Region. On the basis of the analysis of the ϕ,ψ values (data not shown), a helix running from S10 to L20 is identified. This region is well-defined as demonstrated by the low averaged backbone rmsd (⟨rmsd⟩ = 0.36 Å). As evidenced by its hydrogen bond network (13O−17NH, 15O−19NH, and 16O−20NH), the segment W14−L20 is in an α-helix structure (Figure 5a). However, the high $^3J_{NH-H\alpha}$ value of V16 indicates some local distortion. In contrast, the helix type adopted by the segment 10−13 is more difficult to define. The hydrogen bond network (9O−12NH and 11O−14NH) suggests that the conformation of the segment 10−13 is similar to a 3_{10} helix. However, there are still several $d_{\alpha N(i,i+3)}$ connectivities (Figure 3) although they are weak compared to those in the α-helical segment W14−L20. For residue 13, a $^3J_{NH-H\alpha}$ value higher than 6 Hz was observed in CHABII as in the native protein (Bontems et al., 1991a) and in several scorpion toxins (Johnson et al., 1994; Dauplais et al., 1995). Therefore, this distortion is not related to the presence of the Aba residues but seems to be a common feature of the scorpion fold.

β-Sheet and β-Turn Regions. As judged from ϕ,ψ values (data not shown) and the hydrogen bond network (Figure 5a), two antiparallel β-strands, residues R25−M29 and K32−Y36, linked by β-turn residues N30−K31, are characterized. The region from R25 to Y36 is well-defined (⟨rmsd⟩ = 0.38 Å on backbone atoms). The two strands are stabilized by three hydrogen bonds (25O−36NH, 27O−34NH, and 29NH−32O). The turn, as analyzed by the criteria described by Wilmot et al. (1988), is close to a type I β-turn. The abnormally low $^3J_{NH-H\alpha}$ value (smaller than the 5 Hz line

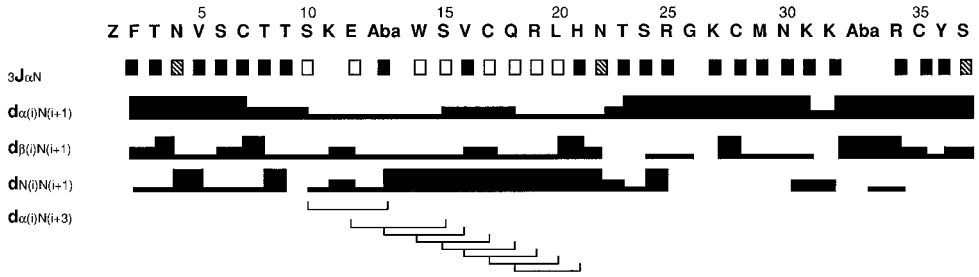

FIGURE 3: Sequence of CHABII and NMR data used for secondary structure identification. The data are derived from NOESY and DQF-COSY spectra at pH 6.3 and 5 °C. $^3J_{\alpha N}$: (open squares) $^3J_{\alpha N} \leq 6$ Hz; (hatched squares) 6 Hz $\leq {}^3J_{\alpha N} \leq 9$ Hz; (solid squares) $^3J_{\alpha N} \geq 9$ Hz.

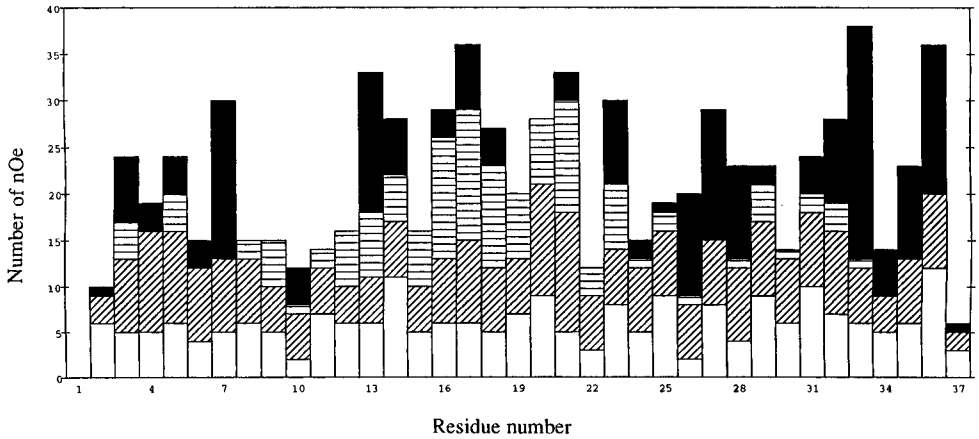

FIGURE 4: Number of NOE connectivities per residue (open squares, intra-NOEs; (diagonally hatched squares, sequential NOEs; (horizontally hatched squares, medium NOEs; (solid squares, long-range NOEs).

Table 1: Structural Statistics[a,b]

⟨*E*(total)⟩	309 ± 8 kcal·mol^{-1}
⟨*E*(bond)⟩	26 ± 1 kcal·mol^{-1}
⟨*E*(angle)⟩	105 ± 4 kcal·mol^{-1}
⟨*E*(dihe)⟩	186 ± 5 kcal·mol^{-1}
⟨*E*(improper)⟩	2.0 ± 0.5 kcal·mol^{-1}
⟨*E*(VdW)⟩	−23 ± 5 kcal·mol^{-1}
energetic cost of deviations from exptl restraints[c]	
⟨*E*(NOE)⟩	13.3 ± 1.5 kcal·mol^{-1}
⟨*E*(cdihe)⟩	0.02 ± 0.01 kcal·mol^{-1}
deviations from idealized geometry	
⟨rmsd(bond)⟩	0.012 Å
⟨rmsd(angle)⟩	2.6°
⟨rmsd(improper)⟩	1.5°

[a] All values were averaged over 30 X-PLOR lowest energy refined structures. [b] The force field used is parallh22x.pro. The van der Waals energy is calculated with a switched Leonard-Jones potential. Electrical energy was not taken into account. [c] The values of squared-well NOE and dihedral angle potentials are calculated with force constants of 20 kcal/(mol·Å^2) and 50 kcal/(mol·rad^2), respectively.

width) for Aba33 indicates a distortion in the β-sheet. This distortion precludes the formation of the hydrogen bond 27NH−34O.

The short N-terminal extended strand (F2−T3) is poorly defined and thus does not form any hydrogen bond with the adjacent β-strand 32−36 (Figure 5a) as observed in the three-stranded β-sheet of ChTX (Bontems et al., 1991a).

Disulfide. The correct pairing of the remaining two disulfides (7−28 and 17−35) in CHABII was checked chemically (Vita et al., 1994). Furthermore, the same structure was converged from a test DIANA calculation without any distance restraint added from the two disulfides, suggesting that the available experimental constraints were sufficient to determine the protein structure. As shown in Table 2, the disulfide 17−35 is well-defined with a good precision in a right-handed conformation (Richardson, 1981). This conformation is one of the most frequently found in protein structures. Disulfide 7−28 is poorly defined, with two conformations which are rarely observed in proteins (Srinivasan et al., 1990). For this disulfide bridge two conformations were accordingly described for several members of the short scorpion toxin family (Bontems, 1992; Dauplais et al., 1995; Meunier et al., 1993).

Side Chains. The side chains of CHABII can be divided into two groups: the side chains that are exposed to solvent and those that are well buried. In general, the solvent-exposed side chains are poorly defined, as indicated from their high rmsd values (>1.5 Å) (Z1, E12, W14, R19, N22, R25, K27, K31, and R34). In contrast, the buried hydrophobic side chains (T3, V5, C7, Aba13, V16, C17, L20, H21, T23, C28, Aba33, and C35) show low rmsd values (<1.5 Å). They have a well-defined orientation with most χ_1 values determined experimentally and they present numerous NOEs (more than 24 per residue) (Figure 4). These 12 side chains constitute a hydrophobic core organized around the two remaining disulfides (Figure 5b): the two Aba with T3, V5, and V16 have a central position sandwiched between the two remaining disulfides. Residues L20, H21, and T23 are located in the loop connecting the helix to the two-stranded β-sheet.

Comparison with ChTX. Figure 5c presents a stereoview of the superimposition of the 10 lowest energy NMR structures of CHABII and ChTX. The averaged backbone rmsd value between CHABII and ChTX, based on a pairwise comparison on the backbone atoms, is 1.44 Å, revealing that the overall structures of the two proteins are very similar even though the two structures are determined under different conditions: 5 °C and pH 6.3 for CHABII and 45 °C and pH 3.5 for ChTX. However, some structural differences are observed, i.e., the N-terminal residues Z1 and K31. The structural perturbation on Z1 is well-correlated to its larger

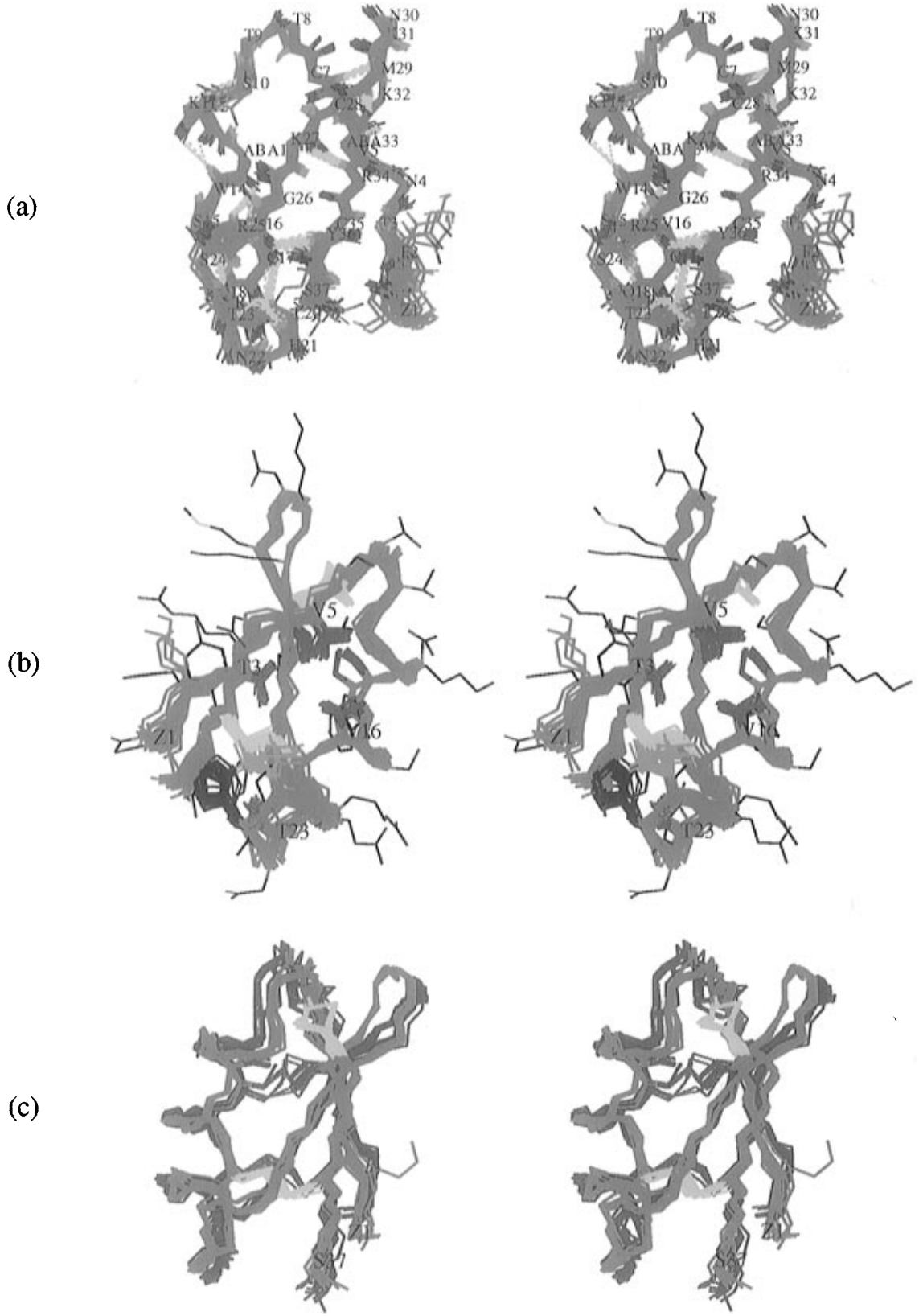

FIGURE 5: (a) Stereoview of the superimposition of 30 refined NMR structures of CHABII, showing the overall structure and hydrogen bond network of CHABII. Different colors are used to indicate different atoms or bonds (green, backbone atoms; red, oxygen; blue, NH; and yellow, hydrogen bond). (b) Stereoview of the superimposition of 30 refined NMR structures fitted with the mean structure of CHABII, showing the side chain packing of residues involved in the hydrophobic core. Different colors are used to indicate different atoms or side chains of residues (green, backbone atoms; yellow, Cys; red, Aba; orange, Val; cyan, Leu; blue, His; purple, Thr). The other side chains are only shown for the mean structure. (c) Stereoview of the superimposition of the 10 best CHABII structures and the 10 best ChTX structures (Brookhaven Protein Data Bank reference 2CRD). Different colors are used to indicate different atoms or side chains of residues (green, backbone atoms of CHABII; red, backbone atoms of ChTX; purple, disulfides in ChTX; yellow, disulfides in CHABII; orange, Aba residues 13 and 33).

Hα chemical shift variation observed (Figure 2). The two remaining chemical shift variations on K11 and G26 are smaller and difficult to correlate to structural variations as they are possibly due to small orientational differences of

Table 2: Conformations of the Two Disulfide Bridges in the 30 NMR Structures of CHABII

			χ angles ± rmsd				
S−S bridges	no. of structures	%	$\langle\chi^1{}_i\rangle$	$\langle\chi^2{}_i\rangle$	$\langle\chi^3{}_{ss}\rangle$	$\langle\chi^2{}_j\rangle$	$\langle\chi^1{}_j\rangle$
Cys7−Cys28	7	13	79 ± 6	151 ± 5	65 ± 5	121 ± 10	96 ± 12
Cys7−Cys28	23	87	175 ± 4	−100 ± 7	−52 ± 3	140 ± 7	54 ± 4
Cys17−Cys35	30	100	−82 ± 6	−96 ± 10	165 ± 19	70 ± 6	−147 ± 5

the side chains not attainable by the present methodology.

The superimposition of the energy-minimized average structures of CHABII and ChTX shows that the rmsd value for the heavy atoms of the buried side chains (the side chains for which the relative surface accessibility is less than 0.5: T3, V5, C7, Aba13, V16, C17, L20, H21, T23, C28, Aba33, C35) is 1.45 Å. This rmsd value decreases to 1.2 Å if residues Aba13, L20, and T23 whose side chains deviate the most are not considered. If one compares only the central residues of the hydrophobic core (T3, V5, V16) (Figure 5b), the side chain rms deviation is 0.7 Å. For the 12 residues which form the hydrophobic core of the protein, 9 present the same rotamer for the χ_1 dihedral angle in CHABII and ChTX. χ_1 rotamer differences concern one Aba and two cysteine residues: (i) Aba13 in CHABII and C13 in ChTX have their side chains in the same orientation for 7 of the 30 structures (Figure 5c); (ii) C28 and C35 have different χ_1 dihedral angles as compared to ChTX, but these differences correspond to only minor variations on the Cβ and Sγ positions (<1.7 Å). In conclusion, the packing of the hydrophobic core is well-preserved although the disulfide 13−33 has been deleted.

DISCUSSION

In the present study, the NMR structure of CHABII, a derivative of ChTX lacking the disulfide 13−33, was determined at 5 °C and pH 6.3 from a large set of NMR constraints (519 distance and 46 dihedral restraints). The NMR structure of CHABII is well-defined as judged from the low averaged backbone atom rmsd value (0.65 Å for the entire sequence and 0.48 Å for segment 3−36).

Comparison of the solution structures of CHABII and ChTX (Bontems et al., 1991a,b) revealed that the deletion of the disulfide 13−33 does not affect the overall structure, indicating that this disulfide is not needed for the α/β motif to fold (Figure 5c). This is all the more striking as the disulfide 13−33 is part of the conserved consensus sequence Cys-x-x-x-Cys-[...]-Cys-x-Cys, which participates to the spacing of the half-cystines that allow the appropriate linkage of the α-helix to the β-sheet of the fold (Bontems, 1992; Bontems et al., 1992). Analogously, experiments made with derivatives of the structurally unrelated BPTI also revealed that deletion of any of the three disulfides did not affect the BPTI fold (States et al., 1984; Eigenbrot et al., 1990; Van Mierlo et al., 1991). In particular, the X-ray study of the most stable BPTI derivative ($[5-55,14-38]_{Ala}$) revealed that this derivative adopted a structure highly similar to that of the native BPTI (Eigenbrot et al., 1990).

Moreover, the present study reveals that the packing of the hydrophobic core that is observed in ChTX is also well-preserved in CHABII. The residues involved in the hydrophobic core are conserved in various proteins adopting this α/β motif and were previously proposed to be associated with the stability of this fold (Bontems, 1992; Bontems et al., 1992). Although the disulfide 13−33 is located within this packing, its deletion does not disrupt the structure of the hydrophobic core. More precisely, no displacement of the main chain of the Aba residues was found (Figure 5c). The distance between their Cα (6.39 ± 0.3 Å) is the same as that in ChTX (6.08 ± 0.4 Å) (difference of the same order as the standard deviation). The intensity of the NOE cross peak between the protons of the methyl group of the Aba side chains yields a distance of 4 ± 0.6 Å between the carbon atoms of these methyls. In the structures, the averaged value of this distance is 3.6 ± 0.5 Å, indicating that these side chains are in close contact without a significant cavity between them. Possibly, introduction of two hydrophobic Aba residues at positions 13 and 33 contributes to maintain the hydrophobic core. Whether conservation of the hydrophobic core is directly associated with the formation of this α/β fold remains to be established. If this proposal proved to be valid, one may anticipate that the tolerance of the fold to mutations in residues within the core will be limited, whereas residues having their side chains on the protein surface will have much greater permissiveness, as observed with other proteins (Bowie et al., 1990; Matthews, 1993).

If substitution of the half-cystines 13 and 33 by Aba residues has little consequence on the overall architecture of ChTX, it mainly reduces its stability and may cause some minor local structural perturbations. The helix is distorted and the β-sheet is less well-defined as compared to ChTX. These small differences could be due to the deletion of the 13−33 disulfide or to the difference between the experimental conditions for the structure determination. Upon deletion of the disulfide 13−33, the stability of the toxin toward various denaturants is clearly reduced (unpublished data). However, experimental conditions were found (pH 6.3 and temperature of 5 °C) to collect enough NMR data to determine the structure. Similar destabilizations were observed with proteins having missing disulfides (Mayr et al., 1994; van Mierlo et al., 1991).

It was previously shown that the deletion of the disulfide 13−33 causes a slight decrease in biological activity. More precisely, the affinity of the derivative for the K^+ channel was only 8-fold lower than that of ChTX (Vita et al., 1994). The strong retention of the activity of CHABII as compared to ChTX agrees well with our observation that the overall structures of the two proteins are the same.

In conclusion, the solution structure of CHABII, a two-disulfide derivative of ChTX, is similar to that of the native protein, indicating that the conserved 13-33 disulfide is unnecessary for the formation of this α/β motif. The conservation of this fold is accompanied by preservation of the hydrophobic core, thus emphasizing the role of hydrophobic interactions in the structural organization even for such a small protein as ChTX. This conclusion agrees with earlier observations on the stabilizing role of hydrophobic interactions (Kellis et al., 1988; Sharp et al., 1991; van den Burg et al., 1994; Butcher et al., 1995; Dill & Stigter, 1995). It further suggests that hydrophobic interaction may be important for the formation of a fold as small as the α/β motif in which most residues are assumed to be exposed to

the solvent. Undoubtedly, these observations will have to be taken into account in proceeding to further engineering of this motif.

ACKNOWLEDGMENT

We thank Drs. L. Remerowski and S. Zinn-Justin for their fruitful comments during the writing of this paper. The DIANA program was provided by Prof. K. Wüthrich and the X-PLOR program by Dr. A. Brünger.

SUPPORTING INFORMATION AVAILABLE

One table containing proton chemical shifts of CHABII at pH 6.3 and 5 °C (2 pages). Ordering information is given on any current masthead page.

REFERENCES

Bonmatin, J. M., Bonnat, J. L., Gallet, X., Vovelle, F., Ptak, M., Reichhart, J. M., Hoffmann, J. A., Keppi, E., Legrain, M., & Achstetter, T. (1992) *J. Biomol. NMR 2*, 235−256.

Bontems, F. (1992) Ph.D. Thesis, Université Paris XI.

Bontems, F., Roumestand, C., Boyot, P., Gilquin, B., Doljansky, Y., Ménez, A., & Toma, F. (1991a) *Eur. J. Biochem. 196*, 19−28.

Bontems, F., Roumestand, C., Gilquin, B., Ménez, A., & Toma, F. (1991b) *Science 254*, 1521−1523.

Bontems, F., Gilquin, B., Roumestand, C., Ménez, A., & Toma, F. (1992) *Biochemistry 31*, 7756−7764.

Bowie, J. U., Reidhaar Olson, J. F., Lim, W. A., & Sauer, R. T. (1990) *Science 247*, 1306−1310.

Braunschweiler, L., & Ernst, R. R. (1983) *J. Magn. Reson. 53*, 521−528.

Bruix, M., Jimenez, M. A., Santoro, J., Gonzalez, C., Colilla, F. J., Mendez, E., & Rico, M. (1993) *Biochemistry 32*, 715−724.

Brünger, A. T. (1992) *X-PLOR version 3.1: A System for X-Ray Crystallography and NMR*, Yale University Press, New Haven and London.

Brünger, A. T., Kuriyan, K., & Karplus, M. (1987) *Science 235*, 458−460.

Butcher, D. J., Bruch, M. D., & Moe, G. R. (1995) *Biopolymers 36*, 109−120.

Chang, J. Y. (1995) *J. Biol. Chem. 270*, 25661−25666.

Coles, M., Munro, S. L. A., & Craik, D. J. (1994) *J. Med. Chem. 37*, 656−664.

Cornet, B., Bonmatin, J. M., Hetru, C., Hoffmann, J. A., Ptak, M., & Vovelle, F. (1995) *Structure 3*, 435−448.

Dauplais, M., Gilquin, B., Possani, L. D., Gurrola-Brions, G., Roumestand, C., & Ménez, A. (1995) *Biochemistry 34*, 16563−16573.

David, D. G., & Bax, A. (1985) *J. Am. Chem. Soc. 107*, 2820−2821.

Dill, K. A., & Stigter, D. (1995) *Adv. Protein Chem. 46*, 59−103.

Drakopoulou, E., Zinn-Justin, S., Guenneugues, M., Gilquin, B., Ménez, A., & Vita, C. (1996) *J. Biol. Chem. 271*, 11979−11987.

Eigenbrot, C., Randal, M., & Kossiakoff, A. A. (1990) *Protein Eng. 3*, 591−598.

Eyles, S. J., Radford, S. E., Robinson, C. V., & Dobson, C. M. (1994) *Biochemistry 33*, 13038−13048.

Ferrer, M., Barany, G., & Woodward, C. (1995) *Nature Struct. Biol. 2*, 211−217.

Gilquin, B., Roumestand, C., Zinn-Justin, S., Ménez, A., & Toma, F. (1993) *Biopolymers 33*, 1659−1675.

Gippert, G. P., Yip, P. F., Wright, P. E., & Case, D. A. (1990) *Biochem. Pharmacol. 40*, 15−22.

Güntert, P., Braun, W., & Wüthrich, K. (1991) *J. Mol. Biol. 217*, 517−530.

Hammen, P. K., Scholtz, J. M., Anderson, J. W., Waygood, E. B., & Klevit, R. (1995) *Protein Sci. 4*, 936−944.

Hyberts, S. G., Marki, W., & Wagner, G. (1987) *Eur. J. Biochem. 164*, 625−635.

Johnson, B. A., Stevens, S. P., & Williamson, J. M. (1994) *Biochemistry 33*, 15061−15070.

Karplus, M. (1963) *J. Am. Chem. Soc. 85*, 2870−2871.

Kellis, J. T., Jr., Nyberg, K., Sali, D., & Fersht, A. (1988) *Nature 333*, 784−786.

Kumar, A., Ernst, R. R., & Wüthrich, K. (1980) *Biochem. Biophys. Res. Commun. 95*, 1−6.

Le-Nguyen, D., Heitz, A., Chiche, L., El Hajji, M., & Castro, B. (1993) *Protein Sci. 2*, 165−174.

Macura, S., & Ernst, R. R. (1980) *Mol. Phys. 41*, 95−117.

Matthews, B. W. (1993) *Curr. Opin. Struct. Biol. 3*, 589−593.

Mayr, L. M., Willbold, D., Landt, O., & Schmid, F. (1994) *Protein Sci. 3*, 227−239.

Ménez, A., Bontems, F., Roumestand, C., Gilquin, B., & Toma, F. (1992) *Proc. R. Soc. Edinburgh 99B*, 83−103.

Meunier, S., Bernassau, J.-M., Sabatier, J.-M., Martin-Eauclaire, M.-F., Van Rietschoten, J., Cambillau, C., & Darbon H. (1993) *Biochemistry 32*, 11969−11976.

Pardi, A., Billeter, M., & Wüthrich, K. (1984) *J. Mol. Biol. 180*, 741−751.

Piantini, U., Sorensen, O. W., & Ernst, R. R. (1982) *J. Am. Chem. Soc. 104*, 6800−6801.

Piotto, M., Saudek, V., & Sklenar, V. (1992) *J. Biomol. NMR 2*, 661−665.

Plateau, P., & Gueron, M., (1982) *J. Am. Chem. Soc. 104*, 7310.

Rance, M. (1987) *J. Magn. Reson. 74*, 557−564.

Rance, M., Sorensen, O., Bodenhausen, G., Wagner, G., Ernst, R. R., & Wuthrich, K. (1983) *Biochem. Biophys. Res. Commun. 117*, 479−485.

Richardson, J. (1981) *Adv. Protein Chem. 34*, 276−330.

Shaka, A. J., & Freeman, R. (1983) *J. Magn. Reson. 53*, 313−334.

Sharp, K. A., Nicholls, A., Fine, R. F., & Honig, B. (1991) *Science 252*, 106−109.

Srinivasan, N., Sowdhamini, R., Ramakrishnan, C., & Balaraam, P. (1990) *Int. J. Pept. Protein Res. 36*, 147−155.

States, D. J., Haberkorn, R. A., & Ruben, D. J. (1986) *J. Magn. Reson. 48*, 286−292.

States, D. J., Dobson, C., M., & Karplus, M. (1984) *J. Mol. Biol. 174*, 411−418.

Trimble, L. A., & Bernstein, M. A. (1994) *J. Magn. Reson. 105*, 67−72.

van den Burg, B., Dijkstra, B. W., Vriend, G., van der Vinne, B., Venema, G., & Eijsink, V. G. H. (1994) *Eur. J. Biochem. 220*, 981−985.

van Mierlo, C. P. M., Darby, N. J., Neuhaus, D., & Creighton, T. E. (1991) *J. Mol. Biol. 222*, 353−371.

Vita, C., Aniort, V., Ménez, A., Toma, F., & Neyton, J. (1994) in *Innovation and Perspectives in Solid Phase Synthesis* (Epton, R., Ed.) pp 201−206, Mayflower Worldwide, Birmingham, U.K.

Vita, C., Roumestand, C., Toma, F., & Ménez, A. (1995) *Proc. Natl. Acad. Sci. U.S.A. 92*, 6404−6408.

Wagner, G., & Wüthrich, K. (1982) *J. Mol. Biol. 155*, 347−366.

Wilmot, C. M., & Thornton, J. M. (1988) *J. Mol. Biol. 203*, 221−232.

Wishart, D. S., Sykes, B. D., & Richards, F. M. (1991) *J. Mol. Biol. 222*, 311−333.

Wüthrich, K. (1986) *NMR of Proteins and Nucleic Acids*, John Wiley, Now York.

Xu, X., & Nelson, J. W. (1994) *Biochemistry 33*, 5253−5261.

Zinn-Justin, S., Roumestand, C., Gilquin, B., Bontems, F., Ménez, A., & Toma, F. (1992) *Biochemistry 31*, 11335−11347.

Zinn-Justin, S., Guenneugues, M., Drakopoulou, E., Gilquin, B., Vita, C., & Ménez, A. (1996) *Biochemistry 35*, 8535−8543.

BI962720H